

## Phosphor settling induced mechanical degradation of silicone/phosphor composite in light emitting diode packages

Xing Chen,<sup>1</sup> Simin Wang,<sup>1</sup> Mingxiang Chen,<sup>1</sup> Sheng Liu<sup>1,2</sup>

<sup>1</sup>School of Mechanical Science and Engineering, Huazhong University of Science and Technology, Wuhan, 430074, China

<sup>2</sup>School of Power and Mechanical Engineering, Wuhan University, Wuhan, 430072, China

Correspondence to: S. Liu (E-mail: victor\_liu63@126.com)

**ABSTRACT:** Silicone/phosphor composite is a functional material used in light emitting diode (LED) packages. In this article, effect of phosphor settling on mechanical properties and microstructure of phosphor/silicone composite is investigated experimentally and numerically. Test samples of silicones with various degrees of phosphor settling were prepared and uniaxial tensile tests were conducted. The results indicate that, for specific volume fraction of phosphor, phosphor sedimentation tends to reduce the strength and elongation of overall composite. And with increasing degree of sedimentation, the weakening effect becomes more significant. The fractographs of the test samples indicate that cracks initiate around the bottom area where phosphor particles settle. Numerical investigations, which were conducted by random unit cell model with graded particle distribution, demonstrate that strain localization and stress concentration are significant where phosphor particles concentrate. It can be concluded that, to reduce mechanical degradation, phosphor sedimentation should be minimized in silicone/phosphor composite for LED packages. © 2015 Wiley Periodicals, Inc. *J. Appl. Polym. Sci.* 2015, 132, 42006.

**KEYWORDS:** composites; degradation; mechanical properties; microscopy; structure; property relations

Received 9 October 2014; accepted 18 January 2015

DOI: 10.1002/app.42006

### INTRODUCTION

White light emitting diodes (LEDs) hold the promise for light-weight, cost-effective and environmental-friendly lighting sources for the next-generation lighting technology and display system.<sup>1–3</sup> In high-power phosphor-converted LED packages, silicone/phosphor composite, which consists of silicone resin and phosphor particles, serves as the key material for light conversion. Nevertheless, as a particle-embedded polymer material, silicone/phosphor composite is vulnerable to mechanical loadings.<sup>4</sup> The fracture of silicone/phosphor composite will result in degradation or even failure of overall LED module.<sup>5–9</sup> Mechanical stability of this material significantly affects the long-time reliability of the LED packages.<sup>10–13</sup> The lack of mechanical properties of silicone/phosphor composite highly limits the quantitative assessment of the reliability of the whole package.<sup>14</sup>

In the state-of-art phosphor-converted LED packages, phosphor particles are randomly dispersed in silicone matrix. Silicone/phosphor composite are coated onto the LED chip for light conversion. It is observed that the phosphor particles tend to settle in the silicone encapsulant during curing process.<sup>15</sup> The graded dispersion of phosphor in the cured silicone matrix will significantly affect the optical, thermal, as well as mechanical properties of the composite. Recent researches involve effect of

phosphor settling on optical and thermal properties of the silicone composite.<sup>16,17</sup> However, mechanical degradation of the silicone encapsulant results from phosphor sedimentation has rarely been covered. This topic is of great significance to the material stability of silicone/phosphor composite and mechanical reliability of whole LED packaging. In the light of this statement, we are motivated to study the effect of phosphor settling on mechanical properties of silicone/phosphor composite.

In this article, a multiscale hierarchical approach is introduced to study the mechanical properties and damage evolution of silicone composite with different degree of phosphor sedimentation. Macro-scale mechanical behavior of the material is obtained by tensile tests, micro-scale fracture surface of the composite is observed by scanning electron microscope (SEM). A quantitative parameter named degree of sedimentation (DoS) is introduced to characterize the settling of phosphor particles in silicone matrix. Moreover, local stress–strain field and damage evolution of the material are simulated with a multisphere random unit cell (RUC) model.<sup>18,19</sup> In our experiments, silicone composite with different degree of phosphor sedimentation were obtained. Four groups of samples were prepared and subjected to tensile loading. During the tensile tests, engineering stress–strain curves of samples are automatically recorded and

**Table I.** Physical Property of Material

Material	Property	Value
Phosphor	Density	4.56 g/cm <sup>3</sup>
	Diameter	(13.0±1.5) μm
Silicone	Density	1.15 g/cm <sup>3</sup>
	Viscosity (Uncured)	3.8 Pa·s

analyzed. Fractographs of samples are investigated using SEM observations. In the simulation part, silicone matrix is simulated with neo-Hookean hyperelastic constitutive model,<sup>20,21</sup> and the interphase region between silicone and phosphor is modeled with cohesive law.<sup>22,23</sup> For certain volume fraction of phosphor in silicone, 20 RUCs with different degrees of sedimentation are generated and simulated. The simulation findings from the unit cell model are compared with experimental results for validation.

## EXPERIMENTAL

In our experiment, four groups of silicone samples with different degrees of phosphor sedimentation were prepared and subjected to the uniaxial tensile loads. Tensile tests were conducted for the silicone/phosphor composite according to ASTM D1708 standard.<sup>24</sup> Dog-bone-shaped samples were prepared and experiment was operated on MTS mechanical test machine. Fracture surfaces of the samples were observed by scanning electron microscope (SEM).

### Sample Preparation

For sample preparation, high transparency silicone from Dow Corning, which is a typical encapsulant designed for LED packaging, was selected as the matrix material. Ce<sup>3+</sup> doped Y<sub>3</sub>Al<sub>5</sub>O<sub>12</sub> (Ce : YAG) powder was adopted as the phosphor filler. Physical properties of silicone and phosphor are listed in Table I.

Volume fraction is an important index that is widely used in the realm of particulate composites.<sup>25</sup> Volume fractions of phosphor in silicone, which indicate the content of phosphor particles in silicone matrix, can significantly affect the mechanical properties of silicone composite. In this article, volume fraction of phosphor in silicone was controlled as 7.05%, which equals to the composite density of 1.39 g/cm<sup>3</sup>. This value is a typical phosphor amount used in white LED packaging. In the process of sample preparation, uncured silicone and YAG phosphor powder were mixed and stirred for 30 minutes with laboratory dispersing homogenizer. Subsequently, the material was placed into a plane mold and put into the vacuum chamber to eliminate bubbles. The silicone/phosphor raw material was divided into four groups. One group of the sample was cured immediately, while other three groups of the samples were left to stand for 1, 3, and 10 hours, respectively. Since phosphor particle would settle in silicone matrix under gravity, and longer standing time could result in higher degree of phosphor sedimentation, this standing process was designed to prepare the silicone/

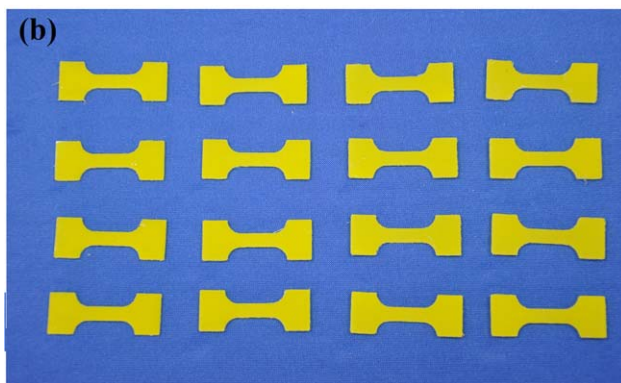
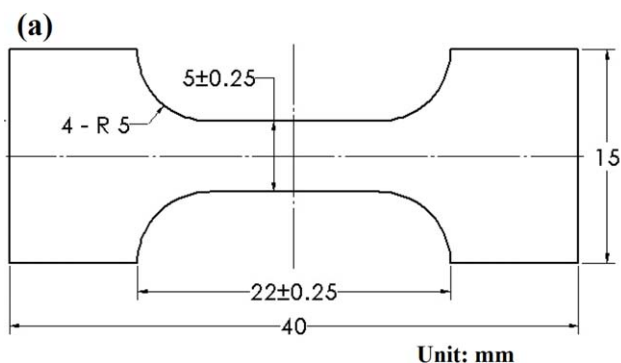


**Figure 1.** (a) Dimensions of test samples. (b) Photograph of test samples. [Color figure can be viewed in the online issue, which is available at [wileyonlinelibrary.com](http://wileyonlinelibrary.com).]

phosphor composite with different degree of phosphor settling. Curing process was conducted at 150°C in thermal chamber for 1 hour. Cured silicone/phosphor composites were mechanically cut to obtain dog-bone-shaped samples for tensile tests. All the samples were carefully smoothed and conditioned according to ASTM D1708 standard to eliminate visible flaws and imperfections, as shown in Figure 1.

### Measurement

Tensile tests were conducted by MTS mechanical test machine, which has a portal frame structure, provides a mechanical testing platform with load range of 500 N and displacement resolution of 0.08 μm. The testing machine was calibrated according to ASTM D638 standard<sup>26</sup> to guarantee accuracy and consistency. Tensile tests of the samples were conducted at speed of 1.2 mm/min at room temperature. Tensile stress–strain curves were automatically recorded by test machine. Fracture surfaces of samples were observed by FEI Quanta 200 scanning electron microscope (SEM) with resolution of 3.0 nm at 30 kV.

### Degree of Sedimentation

In order to characterize the DoS of phosphor particles in silicone matrix, an index of DoS is introduced. To obtain this parameter, the region in silicone/phosphor composite is equally divided into two parts: upper part and lower part. As described in the below equation, DoS denotes degree of sedimentation,  $V_{upper}$  and  $V_{lower}$  denote the volume of phosphor particles in upper and lower regions, respectively:

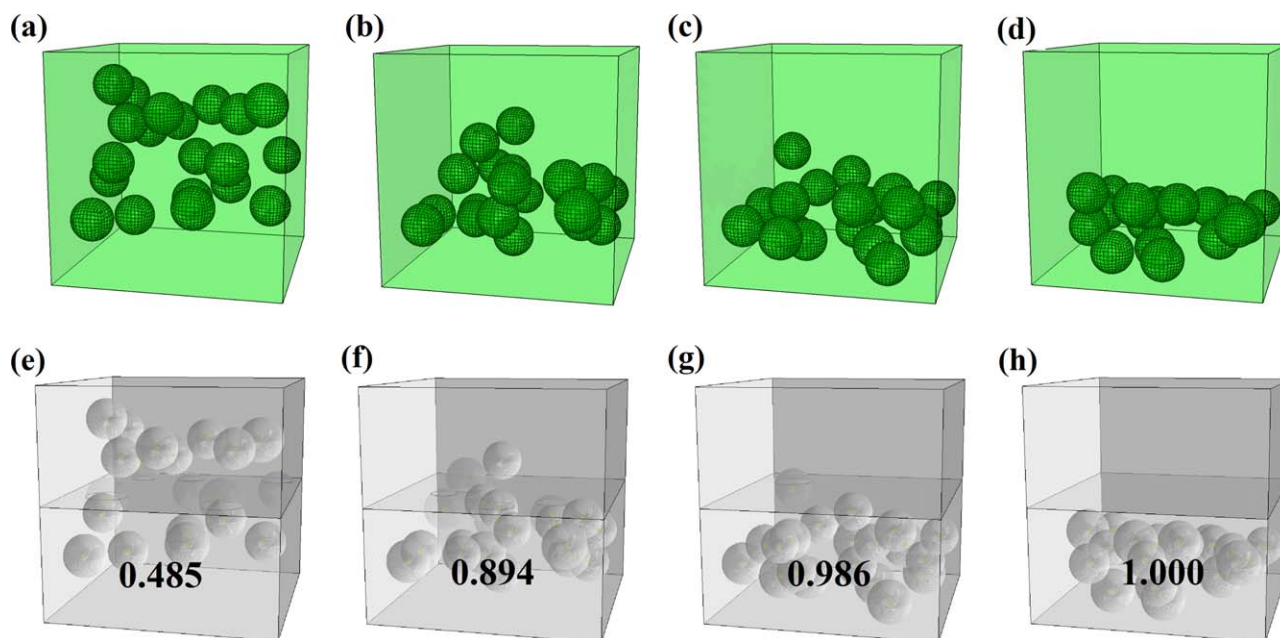


**Figure 2.** Typical unit cell models with different degrees of phosphor sedimentation. The DoS ranges from (a) 0.485 to (d) 1.000. [Color figure can be viewed in the online issue, which is available at [wileyonlinelibrary.com](http://wileyonlinelibrary.com).]

$$DoS = \frac{V_{\text{lower}}}{V_{\text{upper}} + V_{\text{lower}}} = \frac{V_{\text{lower}}}{V_{\text{total}}} \quad (1)$$

This parameter serves as the phenomenological characterization of phosphor sedimentation. When the cross-section image of the composite is obtained through SEM, volumes of particles in upper and lower regions can be calculated. Thus DoS can be obtained subsequently.

## NUMERICAL SIMULATION

### RUC Model

Multisphere RUC model is utilized to simulate the effect of microstructure on mechanical properties of silicone/phosphor composite. In this three-dimensional RUC model, original composite is regenerated with Monte Carlo method, by which randomly dispersed particles are embedded in a statistically representative volume. Twenty RUCs with various degrees of phosphor sedimentation are simulated for a specific volume fraction of phosphor. In the multisphere RUC model, spheres are randomly located inside a unit cube. Phosphor particles are characterized by random dispersed spheres while silicone matrix is represented by the unit cube. Coordinates of centers of particles are generated randomly within the range of the cube.

### Simulation of Phosphor Sedimentation

Since graded distribution of phosphor particles is mainly along vertical direction, the modeling of phosphor sedimentation phenomenon is focused on *Z*-coordinates of particles in the unit cell. In order to simulate phosphor settling phenomenon in RUC model, *Z*-coordinates of the particle centers are calculated as random values distributed by the Gauss law.<sup>27</sup> The mean values of the corresponding Gauss distribution of the coordinates are in accordance with the coordinates of the bottom surface of the unit cell. Standard deviations of random coordinates, which can be regarded as the indicators of the inhomogeneous

distribution, are set at specific values, to construct unit cell model with different degree of phosphor sedimentation, as illustrated in Figure 2(a–d). Meanwhile, *X*- and *Y*-coordinates of particle centers follow uniform distribution. In order to calculate the DoS of the unit cell, the model is partitioned with the middle plane that perpendicular to vertical direction, as shown in Figure 2(e–h). Volumes of particles in upper half and lower half are calculated, thus DoS can be estimated with eq. (1).

### Material Properties

In the RUC model, phosphor particles are modeled as elastic isotropic material. Silicone matrix is modeled as hyperelastic material with neo-Hookean strain energy potential. Nonlinear behavior of silicone can be characterized by this constitutive model.<sup>28</sup> In order to capture the interfacial debonding behavior of the composite, the interphase region between silicone and phosphor is modeled with cohesive law. A progressive damage and failure mechanics model is introduced to simulate the exponential traction-separation behavior of the interphase region.<sup>29,30</sup>

## RESULTS AND DISCUSSION

### Microstructure of Test Samples

The fracture surfaces of different groups of silicone composites were observed by SEM after tensile tests, as shown in Figure 3(a–d). The images were processed by digital image processing software ImageJ V1.47 to identify the shape and location of phosphor particles, as shown in Figure 3(e–h). The degrees of sedimentation of the sample were determined by the area of particles in the lower half over the total area of the particles. It is observed that more phosphor particles concentrate around bottom area of silicone as the DoS of silicone sample increases. Further investigations of samples after tensile tests (Figure 4) indicate that, for silicone composite with highly concentrated

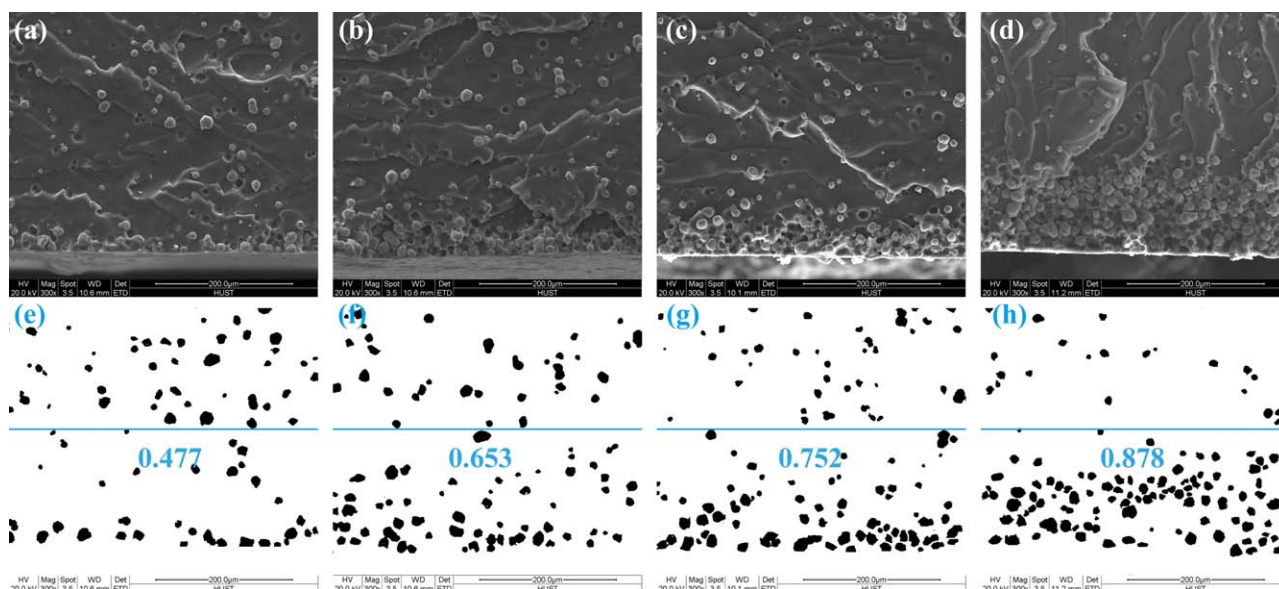


**Figure 3.** (a–d) Fracture surfaces of samples from group 1 to group 4. Images were taken by SEM. (e–h) Shapes and Locations of phosphor particles in silicone matrix. Values of DoS are also presented. [Color figure can be viewed in the online issue, which is available at [wileyonlinelibrary.com](http://wileyonlinelibrary.com).]

phosphor particles, the crack initiates around concentration region and propagates with a radial pattern through the material till final collapse. Highly localized phosphor dispersion and thereby highly concentrated stress status contribute to the reduction of strength of composite. Moreover, intact phosphor particles and voids can be clearly identified, which demonstrate that decohesion of the weak interface between phosphor particle and silicone matrix may be considered as the main failure mechanism. As the degrees of phosphor sedimentation increase, the stress localization and interface decohesion may become more intense, which result in the mechanical degradation of overall silicone/phosphor composite.

### Tensile Properties

Mechanical behaviors of different groups of silicone/phosphor composite are presented in this part. Typical tensile stress–strain

curves of four groups of samples are shown in Figure 5(a). Note that degrees of sedimentation of samples increase from group 1 to group 4, the tensile curves indicate that higher DoS results in lower tensile strength and shorter elongation of the composite. It is worth noticing that nonlinear behavior of silicone become significant at higher phosphor sedimentation. This phenomenon may be explained by the fact that stress distribution in silicone composite with phosphor sedimentation is affected by the highly graded phosphor dispersion, the nonuniform distribution of stress field in silicone result in a nonlinear mechanical response of the material under exterior loadings. Moreover, Young's modulus increases with increasing DoS, as shown in Figure 5(b). The concentrated phosphor particles with high modulus stiffen the overall composite. Figure 5(c,d) demonstrate that phosphor settling can dramatically reduce the strength of the silicone composite, and meanwhile, shorten the

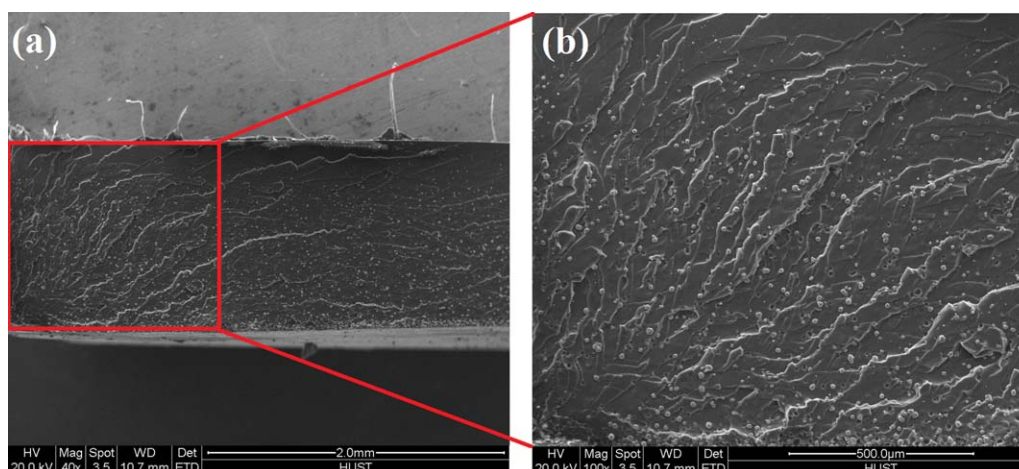


**Figure 4.** Fracture surface of silicone/phosphor composite. The cross section of the fracture surface is observed by SEM after tensile test. The critical location is magnified to emphasize the location of crack initiation. [Color figure can be viewed in the online issue, which is available at [wileyonlinelibrary.com](http://wileyonlinelibrary.com).]

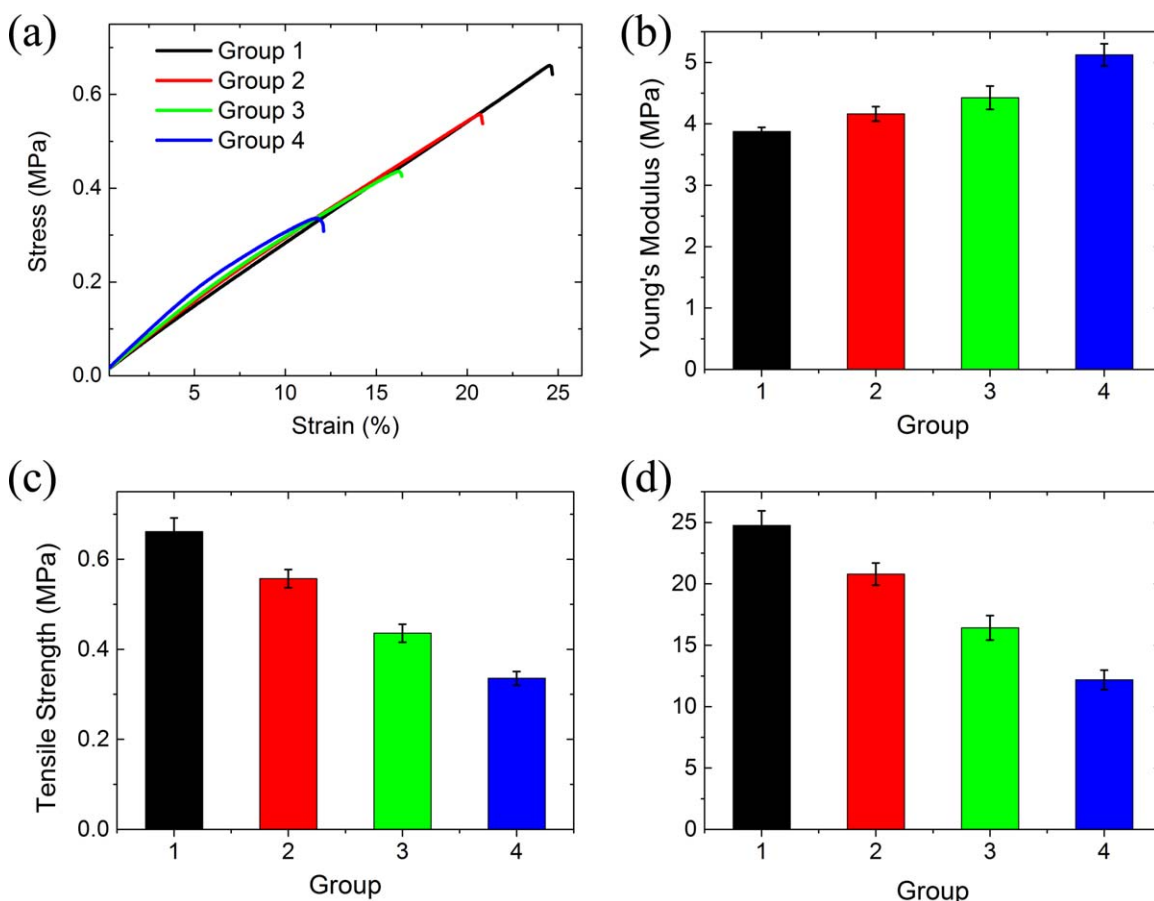


**Figure 5.** Results of tensile tests. (a) Typical stress–strain curves of four groups of samples. (b) Young's modulus, (c) tensile strength, and (d) elongation of test samples. [Color figure can be viewed in the online issue, which is available at [wileyonlinelibrary.com](http://wileyonlinelibrary.com).]

elongation of the material. As the degree of phosphor settling increases, silicone/phosphor composite can be more vulnerable to mechanical loadings.

#### Numerical Investigations

RUC models of silicone composite with different degrees of phosphor sedimentation were generated and employed to investigate the homogenized modulus and distribution of local strain and stress in silicone/phosphor composite. Twenty unit cells were simulated, and DoS of each model was calculated.

#### Homogenized Modulus

The simulation results of effective Young's modulus provided by homogenization method<sup>21–33</sup> are shown in Figure 6. The results indicate that sedimentation of phosphor particles in silicone matrix significantly increase the homogenized modulus of the composite, especially in large DoS. Higher degree of phosphor sedimentation leads to higher effective modulus of overall composite. This tendency is consistent with experimental observations.

#### Local Strain and Stress

In the simulation model, phosphor particles are dispersed in unit cells with various DoS. Figure 7 shows four typical patterns of phosphor dispersion in unit cells and corresponding principal strain fields. When the particles are homogeneously dispersed in the model [Figure 7(a)], the maximum principal strains in the silicone composite are relatively low. As the

particles settle and concentrated around bottom region, the maximum principal strains increase monotonically. Strain localization becomes severe where phosphor particles accumulate. The region with high phosphor concentration is exactly the place with high principal strain. The maximum principal strain and maximum von Mises stress, averaged from simulation

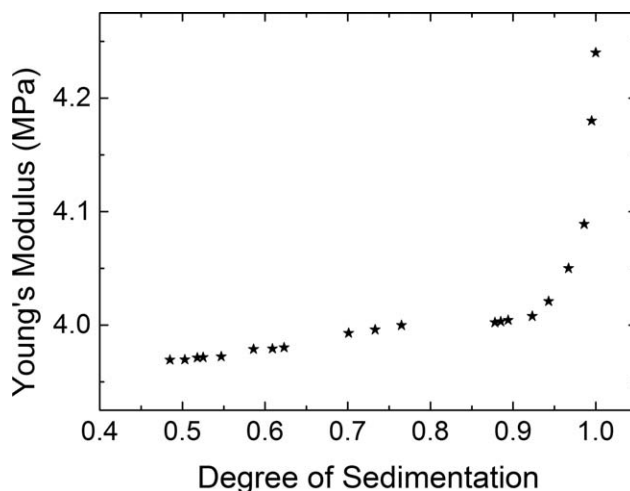


**Figure 6.** Homogenized Young's modulus as a function of degree of phosphor sedimentation.

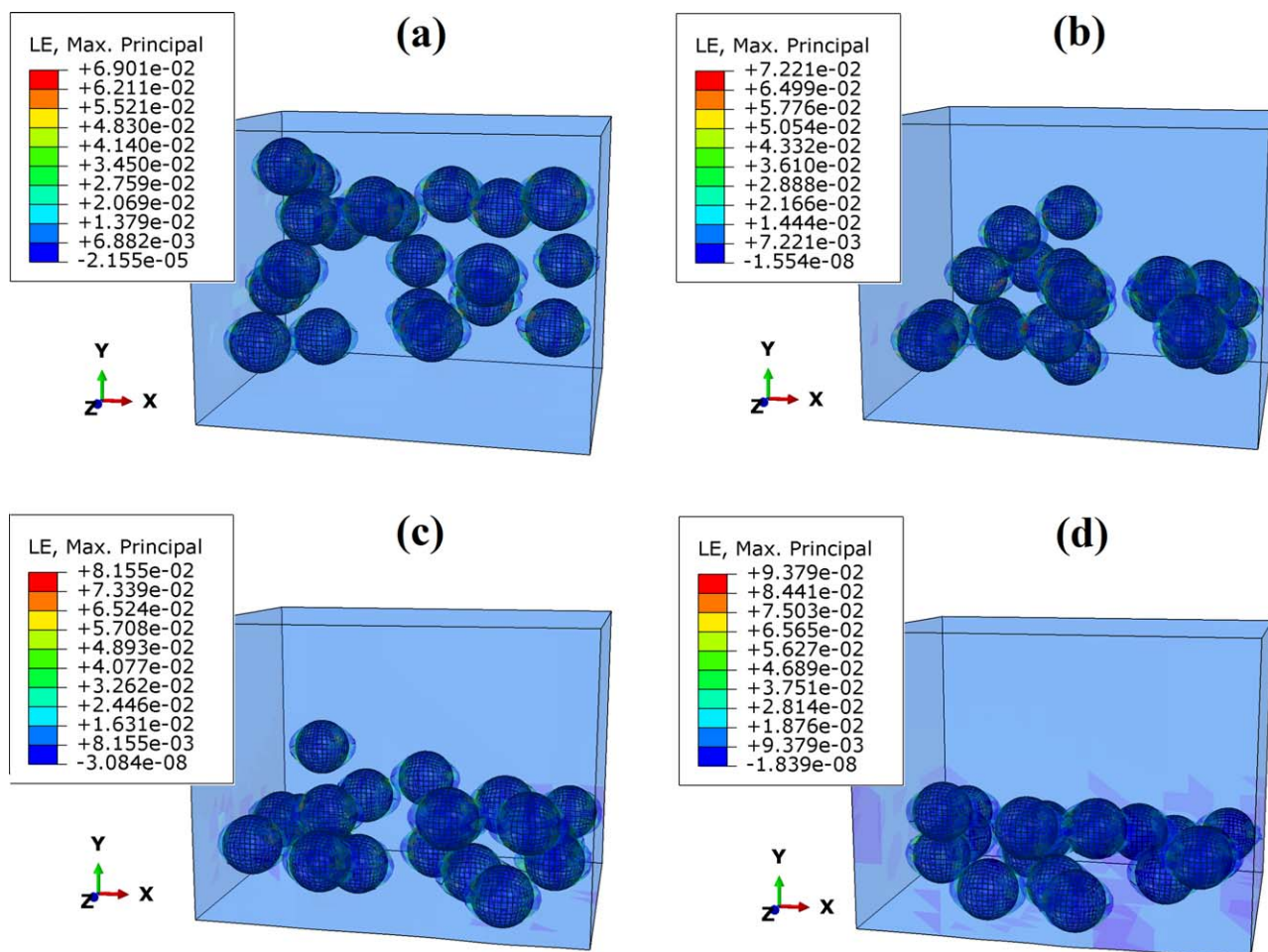


**Figure 7.** Deformed patterns of unit cells with different degrees of phosphor sedimentation. The distribution of principal strain is plotted in the model. [Color figure can be viewed in the online issue, which is available at [wileyonlinelibrary.com](http://wileyonlinelibrary.com).]

results of 20 unit cells, are also plotted as function of degree of phosphor sedimentation in Figure 8. It is shown that strain and stress fields in silicone composite are significantly affected by inhomogeneous dispersion of phosphor particles. High degree

of phosphor sedimentation results in intensified strain localization and stress concentration.

It is worth noticing that strain localization and stress concentration are the main contributors to the interfacial delamination and crack

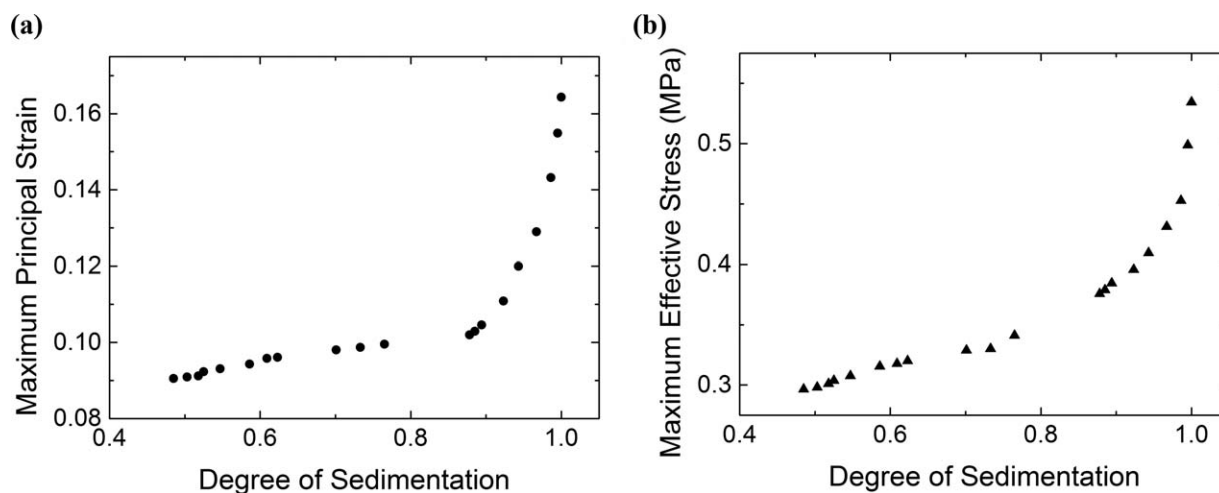


**Figure 8.** Simulation results of (a) maximum principal strain and (b) maximum von Mises stress as a function of degree of phosphor sedimentation.

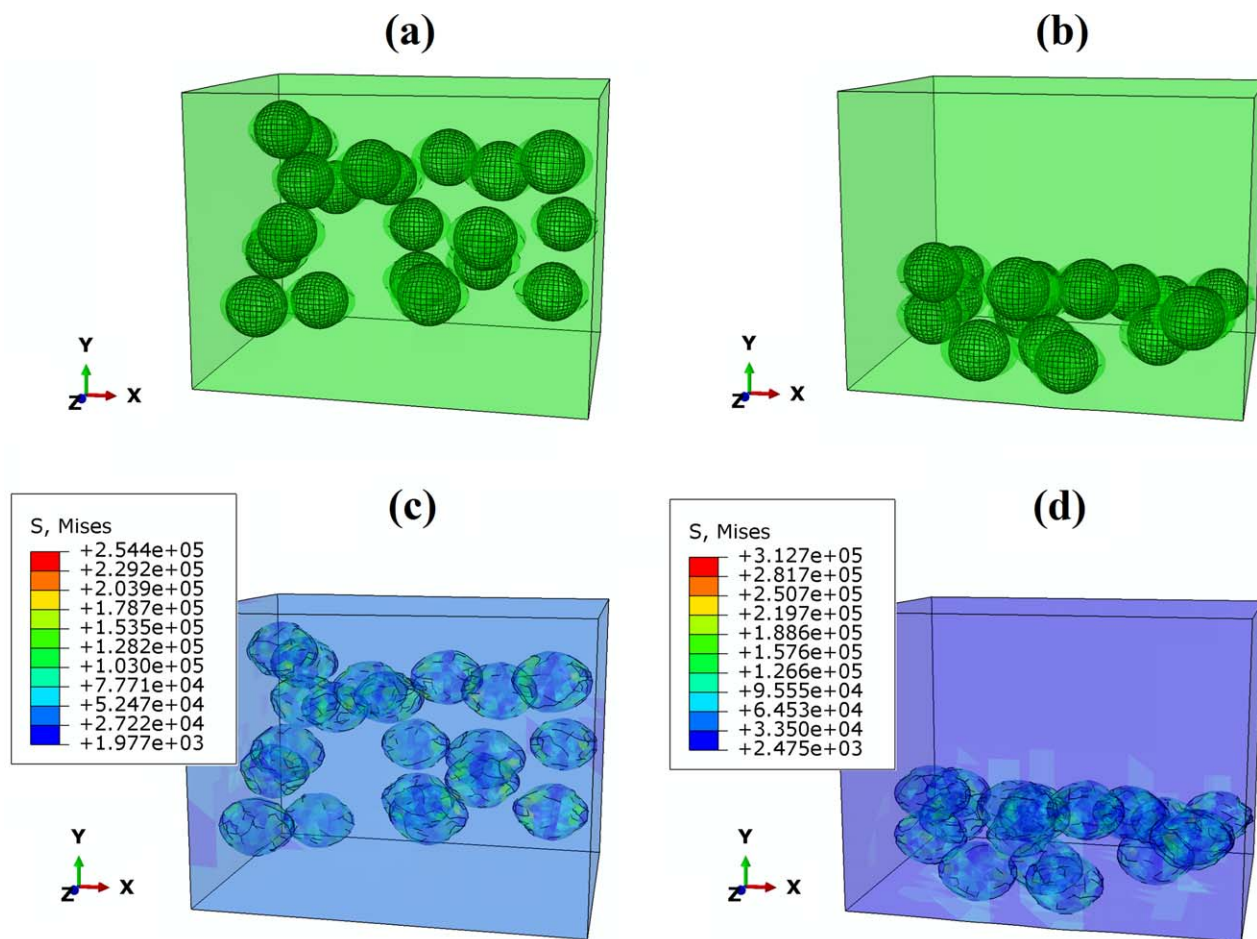


**Figure 9.** Upper Row: Deformed patterns of unit cells with (a) DoS of 0.485 and (b) DoS of 1.000. Lower Row: Distribution of von Mises stress in unit cells with (c) DoS of 0.485 and (d) DoS of 1.000. [Color figure can be viewed in the online issue, which is available at [wileyonlinelibrary.com](http://wileyonlinelibrary.com).]

initiation. As illustrated in Figure 9, high degree of phosphor sedimentation in unit cell leads to stress concentration in the bottom region, which eventually results in interface delamination and crack nucleation around concentrated phosphor particles.

## CONCLUSIONS

In this article, effect of phosphor sedimentation on mechanical properties of silicone/phosphor composite is studied by using a multiscale hierarchical approach. Silicone composites with different degrees of phosphor settling were prepared and subjected to tensile loading. Fracture surfaces of the samples were observed with SEM, while local stress–strain field and damage evolution within the composite were investigated by using multisphere RUC model. The results indicate that phosphor sedimentation leads to increased Young's modulus, reduced strength, and decreased elongation of silicone/phosphor composite. Strain localization and stress concentration are significant where phosphor particles settle, and delamination and cracks nucleate around concentrated particles. With increasing degree of phosphor sedimentation, silicone/phosphor composites become more vulnerable to mechanical loadings. The settling of the phosphor particles in silicone encapsulant can greatly reduce the mechanical stability of the composite, and eventually undermine the reliabil-

ity of the LED package. Therefore, in order to enhance the mechanical stability of the silicone/phosphor composite, phosphor sedimentation in silicone matrix should be minimized. An increased heating rate can be adopted to minimize phosphor sedimentation. Meanwhile, to reduce phosphor sedimentation without increasing internal stress of LED package, the length of cooling stage in curing process should be prolonged so that internal stress can be released at lower cooling rate. The reduction of phosphor sedimentation should not raise other reliability issues in order to produce reliable LED packages.

## ACKNOWLEDGMENTS

This work is supported by National Basic Research Program of China under grant number 2011CB309504, National Natural Science Foundation of China under grant number 51372179 and National Science and Technology Major Project under grant number 2009ZX02038.

## REFERENCES

- Schubert, E. F.; Kim, J. K. *Science* **2005**, *308*, 1274.
- Pimputkar, S.; Speck, J. S.; DenBaars, S. P.; Nakamura, S. *Nat. Photonics* **2009**, *3*, 180.

3. Wang, S. M.; Chen, X.; Chen, M. X.; Zheng, H.; Yang, H. R.; Liu, S. *Appl. Opt.* **2014**, *53*, 8492.
4. Liu, S.; Luo, X. *LED Packaging for Lighting Applications: Design, Manufacturing and Testing*; Wiley: Singapore, **2011**.
5. Luo, X. B.; Wu, B. L.; Liu, S. *IEEE Trans. Device Mater. Reliab.* **2010**, *10*, 182.
6. Chen, Z. H.; Zhang, Q.; Wang, K.; Chen, M. X.; Liu, S. *Microelectron. Reliab.* **2012**, *52*, 1726.
7. Yoon, Y.; Kang, J.; Jang, I.; Chan, S.; Jang, J. *Microelectron. Reliab.* **2013**, *53*, 1519.
8. Tan, L.; Li, J.; Wang, K.; Liu, S. *IEEE Trans. Electron. Packag. Manuf.* **2009**, *32*, 233.
9. Meneghini, M.; Lago, M. D.; Trivellin, N.; Mura, G.; Vanzi, M.; Meneghesso, G.; Zanoni, E. *Microelectron. Reliab.* **2012**, *52*, 804.
10. Chang, M. H.; Das, D.; Varde, P. V.; Pecht, M. *Microelectron. Reliab.* **2012**, *52*, 762.
11. Narendran, N.; Gu, Y.; Freyssonier, J.; Yu, H.; Deng, L. *J. Cryst. Growth* **2004**, *268*, 449.
12. Meneghini, M.; Tazzoli, A.; Mura, G.; Meneghesso, G.; Zanoni, E. *IEEE Trans. Electron Devices* **2010**, *57*, 108.
13. Horng, R. H.; Lin, R. C.; Chiang, Y. C.; Chuang, B. H.; Hu, H. L.; Hsu, C. P. *Microelectron. Reliab.* **2012**, *52*, 818.
14. Liu, S.; Liu, Y. *Modeling and Simulation for Microelectronic Packaging Assembly*; Wiley: Singapore, **2011**.
15. Sommer, C.; Reil, F.; Krenn, J. R.; Hartmann, P.; Pachler, P.; Tasch, S.; Wenzl, F. P. *J. Lightwave Technol.* **2010**, *28*, 3226.
16. Hu, R.; Luo, X. B.; Feng, H.; Liu, S. *J. Lumin.* **2012**, *132*, 1252.
17. Hu, R.; Cheng, T.; Li, L.; Ma, J.; Luo, X. *Int. J. Heat Mass Transf.* **2014**, *77*, 891.
18. Sun, C.; Saffari, P.; Ranade, R.; Sadeghipour, K.; Baran, G. *Compos. A Appl. Sci. Manuf.* **2007**, *38*, 80.
19. Zohdi, T. I.; Wriggers, P. *An Introduction to Computational Micromechanics*; Springer: Berlin, **2008**; Vol. 20.
20. Treloar, L. *Proc. Phys. Soc.* **1948**, *60*, 135.
21. Meunier, L.; Chagnon, G.; Favier, D.; Orgeas, L.; Vacher, P. *Polym. Test.* **2008**, *27*, 765.
22. Hutchinson, J. W.; Suo, Z. *Adv. Appl. Mech.* **1991**, *29*, 63.
23. Kulkarni, M. G.; Geubelle, P. H.; Matous, K. *Mech. Mater.* **2009**, *41*, 573.
24. ASTM, D1708: Standard Test Method for Tensile Properties of Plastics by Use of Microtensile Specimens, ASTM International, **2010**.
25. Chen, X.; Wang, S. M.; Cao, C.; Liu, S. *Compos. Sci. Technol.* **2015**, *107*, 98.
26. ASTM, D638: Standard Test Method for Tensile Properties of Plastics, ASTM International, **2010**.
27. Mishnaevsky, L. L. *Compos. Sci. Technol.* **2006**, *66*, 1873.
28. Treloar, L. *Proc. Phys. Soc.* **1948**, *60*, 135.
29. Inglis, H.; Geubelle, P.; Matous, K.; Tan, H.; Huang, Y. *Mech. Mater.* **2007**, *39*, 580.
30. Williams, J.; Segurado, J.; LLorca, J.; Chawla, N. *Mater. Sci. Eng. A* **2012**, *557*, 113.
31. Hassani, B.; Hinton, E. *Comput. Struct.* **1998**, *69*, 707.
32. Wong, C.; Bollampally, R. S. *J. Appl. Polym. Sci.* **1999**, *74*, 3396.
33. Nemat-Nasser, S.; Hori, M. *Micromechanics: Overall Properties of Heterogeneous Materials*; Elsevier: Amsterdam, **1999**; Vol. 2.